Implications of NbTi Short-Sample Test Results and Analysis for the ITER Poloidal Field Conductor Insert (PFCI)

R. Zanino, M. Bagnasco, W. Baker, F. Bellina, P. Bruzzone, A. della Corte, Y. Ilyin, N. Martovetsky, N. Mitchell, L. Muzzi, A. Nijhuis, Y. Nunoya, K. Okuno, H. Rajainmaki, P. L. Ribani, M. Ricci, E. Salpietro, L. Savoldi Richard, A. Shikov, V. Sytnikov, Y. Takahashi, A. Taran, G. Vedernikov, and E. Zapretilina

Abstract—As the test of the PFCI is foreseen in 2006 at JAERI Naka, Japan, it is essential to consider in detail the lessons learned from the short NbTi sample tests, as well as the issues left open after them, in order to develop a suitable test program of the PFCI aimed at bridging the extrapolation gap between measured strand and future PF coil performance. Here we consider in particular the following issues: 1) the actual possibility to quench the PFCI conductor in the T_{CS} tests before quenching the intermediate joint, 2) the question of the so-called sudden or premature quench, based on SULTAN sample results, applying a recently developed multi-solid and multi-channel extension of the Mithrandir code to a short sample analysis; 3) the feasibility of the AC losses calorimetry in the PFCI.

Index Terms—Fusion reactors, ITER, modeling, superconducting coils.

I. INTRODUCTION

SEVERAL activities have been undertaken in the perspective of the design and construction of the ITER PF coils, which will be based on NbTi conductors. Short (few meter long) but full-size NbTi samples have been tested in the recent past: the PF-FSJS in 2002 [1], and the PFCI-FSJS in 2004 [2], at the SULTAN facility of CRPP Villigen, Switzerland, the BBIII in 2004 [3] at the Toska facility of Forschungszentrum Karlsruhe, Germany.

The PFCI will be the first long (∼50 m) full-size NbTi ITER-like conductor [4]. The PFCI strands were produced in the Bochvar Institute (RF) in accordance with the ITER requirements. Cabling was performed in the Institute for Cabling

R. Zanino, M. Bagnasco, and L. Savoldi Richard are with Dipartimento di Energetica, Politecnico, Torino, Italy (e-mail: roberto.zanino@polito.it).

W. Baker, H. Rajainmaki, and E. Salpietro are with EFDA, Garching, Germany.

F. Bellina is with Universita', Udine, Italy.

P. Bruzzone is with CRPP, Villigen, Switzerland.

A. della Corte, L. Muzzi, and M. Ricci are with ENEA, Frascati, Italy.

Y. Ilyin and A. Nijhuis are with Twente University, Enschede, Netherlands.

N. Martovetsky is with LLNL, Livermore, CA 94550 USA.

N. Mitchell and Y. Takahashi are with ITER IT, Naka, Japan.

Y. Nunoya and K. Okuno are with JAERI, Naka, Japan.

P. L. Ribani is with Universita', Bologna, Italy.

A. Shikov and G. Vedernikov are with Bochvar Institute, Moscow, Russia.

V. Sytnikov and A. Taran are with the Institute for Cabling Industry, Moscow, Russia.

E. Zapretilina is with Efremov Institute, St. Petersburg, Russia.

Digital Object Identifier 10.1109/TASC.2006.873318

Industry (RF) with following jacketing in Ansaldo (Italy). For a sketch of the PFCI as well as other information, which will not be repeated here, we refer to [4].

The main objectives of the PFCI test can be summarized as: (1) establish the DC current sharing limits of the conductor, especially where they are driven below the usual 10 $\mu V/m$ level and compare to predictions based on short (and sub-size) sample tests; (2) measure the overall AC (coupling) losses at various operating conditions (and again compare to short sample measurements); (3) check the effect of cycling on (1) and (2), especially noting the very long term cycling effects predicted by mechanical simulations; (4) investigate stability to fast ramping of the current; (5) investigate the quench behavior.

Here we consider the issues of DC performance assessment (T_{CS}/I_C test), providing a new multi-solid and multi-channel analysis of the results of the PFCI-FSJS. This will contribute to the validation of one of the tools, which we plan to apply in the near future to the PFCI DC performance assessment, including the analysis of the possible effects of long length at peak field [4], peculiar of the PFCI. Also, the feasibility of the Tcs tests from a thermal-hydraulic point of view is considered here, as well as predictions for the calorimetry of the PFCI during the tests of conductor and joint AC losses.

II. STATUS OF COIL MANUFACTURING

The PFCI dummy coil was impregnated in September 2004, but large areas showed a complete lack of impregnation due to a problem of temperature control. This was eventually resolved but caused significant delay. The PFCI coil is now wound, the terminations and the intermediate joint (IJ) formed and completed, see Fig. 1. The instrumentation that is applied to the conductor inside the primary insulation has been assembled, the conductor insulation applied, the GRP filler pieces assembled and the 10 mm glass over-wrap applied. The forward wire (toward the upper busbar) of the voltage tap VT02 was lost during this process, but because of the delays already accumulated it was decided to go ahead. The primary impregnation of the PFCI coil was thus completed in August 2005.

A high resistance joint was observed during the PFCI-FSJS test [2]. For the PFCI IJ (see Fig. 2) the high resistivity of the CuCrZr sleeve was improved by over-aging the sleeve at 550°C for 6 hours. This resulted in improved resistance while not significantly affecting the mechanical properties. The strand-to-sleeve contact resistance was improved by Sn/Pb
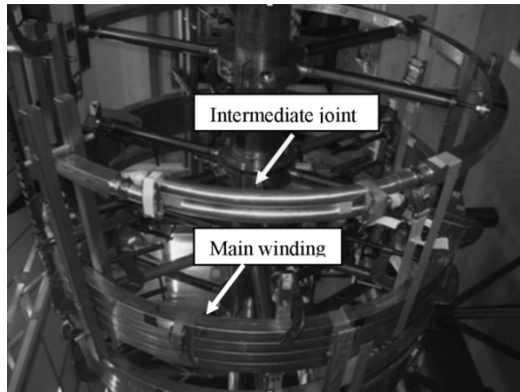
Fig. 1. Part of the PFCI coil with intermediate joint positioned. The coil (738 mm radius) will be inserted in the CSMC bore at the JAERI facility in Naka, Japan. Coolant flow will be from bottom to top.
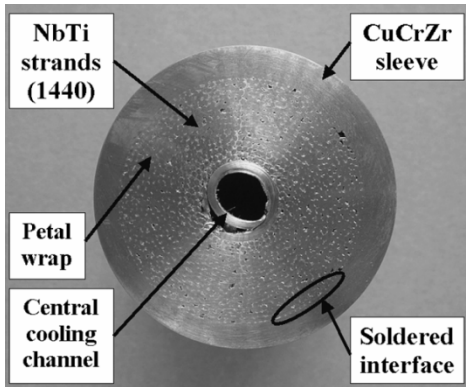

Fig. 2. Conductor cross section at the PFCI intermediate joint. The inner diameter of the central channel is 10 mm.

Fig. 3. Schematic of the apparatus for calibration of the inductive heater.

solder coating the strands and Sn/Pb paste coating the sleeve inner surface, which allows flow of Sn/Pb and thus the formation of meniscus between the strand and the sleeve surface during the heat treatment. The improvements were verified as described in [2]. As a consequence, the expected joint resistance in the PFCI IJ is reduced by 50% with respect to the PFCI-FSJS, to about 5 nΩ. Of course, the joint resistance difference will also introduce some differences between PFCI-FSJS and PFCI test results under comparable operating conditions.

Calibration of the inductive heater (IH) to be used for stability and quench tests will be done separately from the PFCI experiment. A scheme of the apparatus for the calibration is shown in Fig. 3. The apparatus is installed in the magnetic field of a dipole magnet so that the environment should be the same as for the PFCI. Energization of the IH mounted on short length conductor samples produces evaporated He gas in liquid helium (LHe). The amount of energy is evaluated by measuring the volume of the gas using a LHe level meter. The calibration will be performed by the resistive heater, which is placed aside near the conductor sample.

Pick-up coil/magnetization calibration for the IJ AC losses is also planned but details are still under definition.
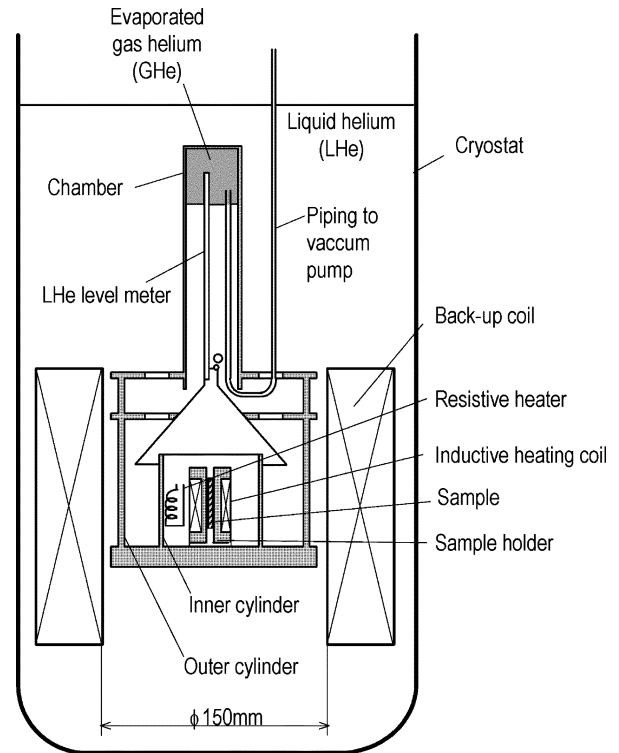
III. FEASIBILITY OF T_{CS} TESTS

In view of the possibly relatively high resistance of the IJ, it is not guaranteed a priori that during T_{CS} tests (driven by the helium heater located at the conductor inlet [4]) the normal zone can be initiated in the main winding as requested (thus allowing the measurement of the critical properties of the conductor), instead of in the IJ or in the upper bus bar.

To check this issue, preliminary *purely thermal-hydraulic* simulations of T_{CS} tests at $I_{PFCI} = 45$ kA, $I_{CSMC} = 21$ kA (background magnetic field $= 6$ T) have been performed with the M&M code [5]. Both the main winding and the bus bar have been simulated, accounting for the heat transfer and heat generation in the IJ (whose resistance is conservatively assumed equal to 10 nΩ). Three different rates: 2 mK/s, 1 mK/s and 0.5 mK/s, are considered for the inlet helium heating, mimicking a slow multi-step (staircase) heating strategy, as applied in the past to other ITER Insert and Model Coils [6]. The helium in the bus bar is kept at 4.5 K. For the critical properties of the NbTi strands, the ITER Design Criteria and the set of parameters suggested in [4] have been adopted. The magnetic field maps are also as in [4].

The results of the simulations show that the current sharing condition is always reached first in the main winding. The T_{CS} location approaches the lower termination as the heater ramp rates become faster.

IV. THE QUESTION OF SUDDEN QUENCH

The problem of a sudden quench of the conductor during T_{CS} tests is somehow ubiquitous in the case of NbTi CICC and related to a high magnetic field gradient on the conductor cross

section, due to the self field [1], [2], [7]. When this phenomenon occurs at temperature/current values lower than expected from single strand measurements, as in the PFCI-FSJS, it may be qualitatively explained as a local quench induced by a highly uneven current distribution, with a strand overload (at locally high electric field) that can hardly be re-distributed because of a low inter-strand voltage. Although some aspects of the sudden quench can be described by simple models [7], using ad-hoc values for some input parameters—typically the heat transfer coefficient h_{St-He} between strands and helium—and simplifying assumptions, e.g., neglecting heat conduction along the strands, a fully self-consistent description is still beyond the present code simulation capabilities [8].

Indeed, the self-consistent modeling of a local quench at the strand level requires in principle a very detailed thermal-(hydraulic) and electric description of the cable. As a first step in that direction, the Mithrandir code [9] has been extended to allow the simulation of the temperature evolution of arbitrary number of strands or cable elements (CE), coupled together as well as with an arbitrary number of hydraulic channels. The current in each CE is assumed constant in time, i.e., the current redistribution is not included in the present model.

Simulations of the PFCI-FSJS left leg (with petal wraps, i.e., the leg more relevant for the PFCI) have been performed with two different levels of discretization of the cable cross section: 1) 6 CE, i.e., the petals; 2) 18 CE, i.e., a nested discretization of the cable cross section, with the petal containing the strand at peak magnetic field (not necessarily the "most loaded" strand if the current is nonuniform) discretized down to the strand level (the $3 \times 4 \times 4 \times 5 \times 6$ multi-stage structure of the PFCI cable giving rise in this case to $[3 + (4 - 1) + (4 - 1) + (5 - 1) + (6 - 1)]$ CE), see Fig. 4(a). The twist pitch of each cabling stage is accounted for. From the hydraulic point of view, six hydraulic channels (i.e., the six petals) have been considered (central channel blocked in these tests). The heat transfer coefficient between the CE and the helium has been conservatively assumed to correspond to the laminar value of Nusselt number $Nu = 4$ (actually valid for circular pipes only), while the contact heat transfer coefficient between the different CE has been assumed to be $50 \, W/m^2K$. The (Bochvar) fit of the strand critical properties is chosen as in [8] and the n index is taken from [10].

The current distribution among the CE has been computed by the THELMA code [11]. In particular, THELMA models the joint and terminations as an equivalent electrical lumped network where the contacts among CE and between CE and resistive saddle are found starting from a geometrical representation of the CE middle lines; the electrical parameters required (contact conductances) are taken/fixed from other independent measurements [12]. While the computed current distribution at the petal level is almost uniform (almost perfect theoretical joint at this level), a nonuniformity of up to $\sim 100\%$ is computed *inside* the most loaded petal by the 18 CE model. A cross check of the computed current distribution has been performed comparing it with the measured magnetic field at the Hall Probe head HP3 (located in the peak field region of the sample), see Fig. 4(b).

Results of the DC performance analysis of the left leg of the PFCI-FSJS during a T_{CS} test at 60 kA and $B_{SULTAN} = 5 \, T$
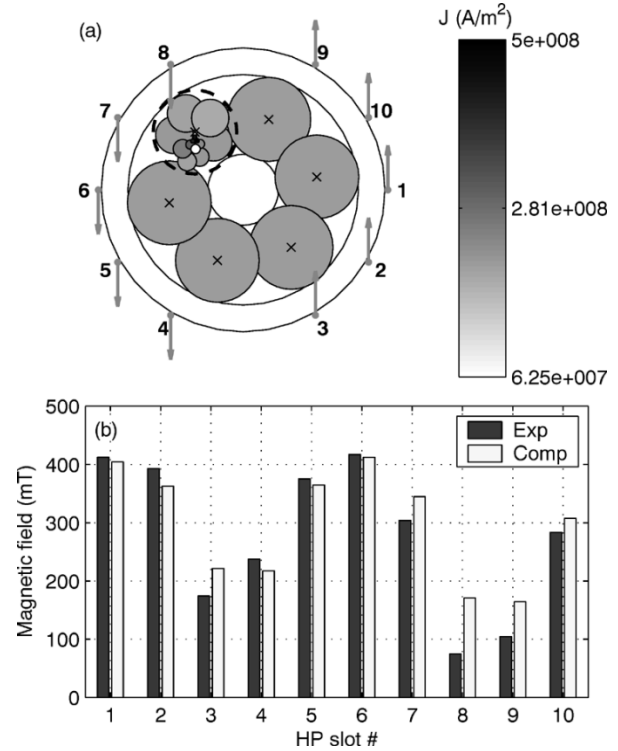

Fig. 4. (a) Schematic view of the computed current density distribution among the 18 CE under Hall Probe head HP3. (b) Measured vs. computed HP3 signals at steady state ($T = 5.3 \, K$), for a total transport current of 60 kA.

are reported in Fig. 5 in terms of electric field-jacket temperature characteristic. The measured characteristic shows that the electric field E_q (voltage/length) at the quench ("vertical" characteristic) is lower than the critical field $E_c = 10 \, \mu V/m$, i.e., the signature of a sudden quench [2]. The computed electric field E_{ave} (averaged along the high field region and across the cable cross section) using 6 CE and/or 18 CE is also reported in Fig. 5, together with the peak electric field E_{peak} computed on the strand at the peak magnetic field. The refinement from 6 to 18 CE leads to a significant improvement in the agreement with the experiment ($\sim 0.25 \, K$ best error in the take-off temperature). For the key parameter E_{peak}/E_{ave} at $E_{ave} = E_c$ [13], we compute $E_{peak}/E_c \sim 2 \times 10^4$ with 18 CE, while this ratio drops to ~ 2.5 in the case of 6 CE. With 18 CE, the early rise of E_{peak} quickly overwhelms its limited weight on the computation of E_{ave}, while the jacket and He temperature remain substantially constant. This explains why a sudden quench is computed with 18 CE, whereas a smooth transition is computed with 6 CE, because all petals reach the critical condition more or less at the same time. Note also that the spikes in the measured voltage [14] are not reproduced, requiring a more detailed discretization level of the cable cross section and the modeling of current redistribution among the CE.

Simulations at 45 kA and 20 kA were also performed (not shown here) within the same framework as discussed above and using the same (frozen) input parameters. The measured take-off temperature is overestimated by $\sim 0.2 \, K$ and $\sim 0.05 \, K$, respectively, when the 18 CE model is used. At all current levels, these results represent an improvement with respect to
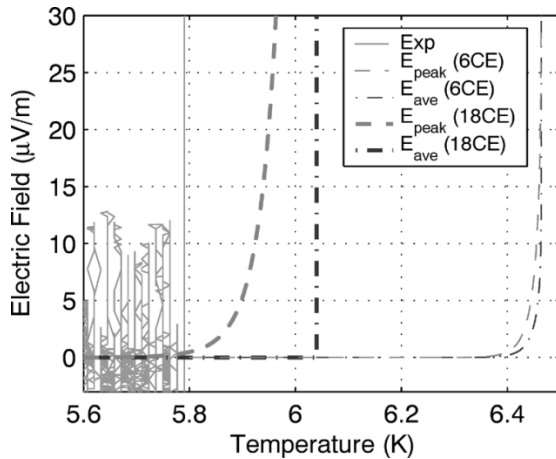
Fig. 5. PFCI-FSJS T_{CS} test at 60 kA, 5 T (# PCD070 409): experimental (solid) vs. computed E-T characteristics in the left leg using the 6 CE model (thin lines) and/or the 18 CE model (thick lines). The experimental data are obtained by dividing the measured voltage signal LV10LV15 by the distance between the voltage taps (0.42 m) and applying a 25 pts moving average.

previous analysis [8]. However, a fully self-consistent and satisfactory picture is still to be achieved (see Fig. 5) and a validated code will be eventually desirable for realistic predictions for the PFCI.

V. CALORIMETRY OF AC LOSSES

The experimental feasibility of the calorimetry of AC losses is related to two issues: 1) sufficiently large temperature increase to be measurable; 2) sufficiently small temperature difference between central channel and annular region (as only the jacket temperature is measured). While the first issue will be assessed experimentally, the second has been numerically investigated with the M&M code.

For the *conductor*, two reference scenarios of the test program are considered: a) exponential discharge of the CS Model Coil from 21 kA, with a time constant $\tau = 6$ s, and b) trapezoidal pulse between 0 and 21 kA with a field ramp rate of 0.5 T/s, both with zero current in the PFCI. Only the coupling losses are considered in view of the relatively fast transients and approximated as uniform along the main winding. Based on the simulation results, the error induced in the calorimetry by the nonhomogeneous temperature distribution on the cross section (hole helium colder than bundle helium) should be $< \sim 5\%$ in these cases.

Concerning the *joint*, the reference scenario of the CS Model Coil exponential discharge from 21 kA ($\tau = 20$ s) with zero current in the Insert has been simulated, varying parametrically the thermal coupling between hole and bundle. The computed temperature difference between hole and bundle at the location of the temperature sensor TS05H (~ 1 m downstream of the IJ) appears significant (up to 0.25 K in the worst case), leading to an overestimation of the losses up to 30%, but a resistive heater

is installed on the IJ to allow an experimental check of the IJ calorimetry.

VI. CONCLUSIONS AND PERSPECTIVE

The PFCI manufacturing has progressed, albeit with some delay, toward the expected test in 2006.

Some of the implications of previous NbTi short sample tests for the PFCI have been considered by analysis here: purely thermal-hydraulic modeling shows that during Tcs tests current sharing is reached first in the conductor, as desired, independently of the IJ resistance; a new model has been developed and applied to the DC performance assessment of the PFCI-FSJS, showing improved results; calorimetry of PFCI conductor AC losses appears accurate while larger errors could be present for the IJ.

A comprehensive action involving all interested laboratories is going to be launched before the tests, for the predictive analysis of different items of the PFCI test program, using validated models/codes.

REFERENCES

[1] D. Ciazynski *et al.*, "Test results on the first 50 kA NbTi full size sample for the international thermonuclear experimental reactor," *Supercond. Sci. Technol.*, vol. 17, pp. 155–160, 2004.

[2] P. Bruzzone *et al.*, "Test results of the ITER PF Insert conductor short sample in SULTAN," *IEEE Trans. Appl. Supercond.*, vol. 15, pp. 1351–1354, 2005.

[3] R. Zanino *et al.*, "Current distribution measurement on the ITER-type NbTi bus bar III," *IEEE Trans. Appl. Supercond.*, vol. 15, pp. 1407–1410, 2005.

[4] ——, "Preparation of the ITER poloidal field conductor insert (PFCI) test," *IEEE Trans. Appl. Supercond.*, vol. 15, pp. 1346–1350, 2005.

[5] L. Savoldi and R. Zanino, "M&M: multi-conductor mithrandir code for the simulation of thermal-hydraulic transients in super-conducting magnets," *Cryogenics*, vol. 40, pp. 179–189, 2000.

[6] R. Zanino *et al.*, "Analysis and Interpretation of the Full Set (2000–2002) of Tcs tests in conductor 1 A of the ITER central solenoid model coil," *Cryogenics*, vol. 43, pp. 179–197, 2003.

[7] R. Wesche *et al.*, "DC performance of subsize NbTi cable-in-conduit conductors," *IEEE Trans. Appl. Supercond.*, vol. 14, pp. 1499–1502, 2004.

[8] D. Ciazynski *et al.*, "DC performances of ITER NbTI Condutcors: models vs. measurements," *IEEE Trans. Appl. Supercond.*, vol. 15, pp. 1355–1358, 2005.

[9] R. Zanino *et al.*, "A two-fluid code for the thermohydraulic transient analysis of CICC superconducting magnets," *J. Fus. Energy*, vol. 14, pp. 25–40, 1995.

[10] L. Zani *et al.*, "Task TW1-TMC/SCABLE: Final report on characterization of NbTi strands representative for the ITER PF coils," AIM/NTT-2004.005, Feb. 2004.

[11] F. Bellina *et al.*, "Superconductive cables current distribution analysis," *Fus. Eng. Des.*, vol. 66–68, pp. 1159–1163, 2003.

[12] ——, "Electromagnetic analysis of superconducting cables and joints in transient regime," *IEEE Trans. Appl. Supercond.*, vol. 14, pp. 1356–1359, 2004.

[13] R. Wesche *et al.*, "Sudden take-off in a large NbTi conductor: not a stability issue," *Adv. Cryo Eng.*, vol. 50 B, pp. 820–827, 2004.

[14] P. Bruzzone *et al.*, "Anomalies on V-I characteristic of NbTi cable-in-conduit conductors," presented at the *SOFT 2004*, Venice, Italy.